

RESEARCH ARTICLE | MAY 10 2013

Aerosol radiative forcing over liquid water clouds based on A-Train synergies and active/passive polarized observations

FREE

D. Josset; L. Doppler; F. Waquet; G. Seze; J. Pelon; Y. Hu; J. Fischer; F. Ravetta; C. Tsamalis; P. Zhai



AIP Conf. Proc. 1531, 436–439 (2013)

<https://doi.org/10.1063/1.4804800>



Boost Your Optics and Photonics Measurements

Lock-in Amplifier

Zurich Instruments

Find out more

Boxcar Averager

Aerosol Radiative Forcing over Liquid Water Clouds Based on A-Train Synergies and Active/passive Polarized Observations

D. Josset^a, L. Doppler^{b,c}, F. Waquet^d, G. Seze^e, J. Pelon^b, Y. Hu^f, J. Fischer^c,
F. Ravetta^b, C. Tsamalis^e and P. Zhai^a

^aSSAI/NASA Langley Research Center, Hampton, VA 23681, USA

^bUPMC/LATMOS 4, Place Jussieu, 75252, Paris, France

^cFreie Universität Berlin, Institute for Space Science, Kaiserswerther Str. 16-18, 14195 Berlin, Germany

^dLaboratoire d'Optique Atmosphérique / CNRS Lille, France

^eLaboratoire de Météorologie Dynamique / IPSL / CNRS, Paris, France

^fNASA Langley Research Center, Hampton, VA 23681, USA

Abstract. We used the A-Train observations as inputs of the Matrix Operator Model to study the effect of aerosol forcing above bright liquid water clouds in the Gulf of Guinea and to determine the vertical profile of heating rates within the aerosol layer. Special emphases are put on recently developed polarization based methodologies. METEOSAT geostationary observations are used to estimate the diurnal variation of the cloud cover.

Keywords: Polarization, Lidar, Aerosols, Clouds.

PACS: 42.68.Jg - 42.68.Ge

INTRODUCTION

Strong radiative forcing is induced by absorbing aerosol overlying low level clouds [1, 2]. It leads to a local change of the earth albedo due to the radiative interactions of the aerosol and clouds layers and to a local warming effect in the aerosol layer [3]. There are few regions around the world where this impact may be significant at the regional scale. It is the case of biomass burning particles transported over the Atlantic West of central Africa above bright stratocumulus clouds.

Although the general physical process of this interaction is well understood in terms of direct forcing, its effect on the climate system is largely uncertain. This is due to the lack of accurate global scale observations of the aerosol optical parameters above the clouds [4], and the need to account for time and space variations of the aerosols and cloud properties in the analysis. Only limited regional in-situ measurements [5] and satellite data analysis [6] have been performed. Moreover, the retrieval of cloud properties is biased by the presence of aerosol above the clouds.

The new developments combining polarized active (CALIPSO [7]) and passive (PARASOL [8]) observations offer the opportunity to retrieve the properties of aerosol above the clouds with an accuracy difficult to achieve by a standard inversion of the lidar data or an analysis of the unpolarized radiance.

The goal of this study is to use those new A-Train products based on polarization as input in the radiative transfer Matrix Operator Model (MOMO [9]) to estimate the radiative forcing of biomass burning along with the associated vertical repartition of the shortwave flux and modification of the heating rate. As the A-Train is performing measurements of the earth surface at a given location only once a day, it is important to understand the representativity of its observations. Geostationary observations are well suited for this purpose and allow us to assess the effect of cloud diurnal variations. We started to study the impact of the cloud diurnal variations on the radiative forcing with the geostationary observations of METEOSAT.

We will describe the tools and the methodology we have used and present and discuss preliminary results for a case study.

The Matrix Operator Model (MOMO)

MOMO [9] is the computer code used to calculate the light field in the stratified atmosphere-ocean system. The code is based on the matrix-operator method and includes multiple scattering with the help of an adding-doubling method. Gas absorption is computed using a non-correlated k-distribution method [10]. During the code development, special emphasis was put on the methods employed to ensure numerical accuracy and energy conservation. The code has been validated by comparing model predictions with the analytical solution of the radiative transfer equation for a semi-infinite Rayleigh scattering atmosphere and by a model inter-comparison for selected problems of the radiative transfer in the atmosphere-ocean system [9].

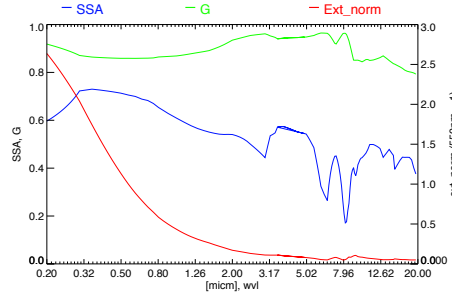


FIGURE 1. Normalized extinction, the asymmetry parameter and single scattering albedo as a function of the wavelength in micrometer.

The aerosol type we used is a modified continental polluted model of OPAC (Optical Properties of Aerosols and Clouds [11] with 10% more soot. The aerosol contains the following components: water soluble (21.4%), insoluble (0.12%), and soot (78.6%). A Mie code determines the phase function and single scattering albedo. Fig. 1 shows the normalized extinction, the asymmetry parameter and the single scattering albedo (SSA) wavelength dependency. The SSA is in the lower boundary of the [5] simulations and we would rather expect a single scattering albedo around 0.8-0.9 at visible wavelength. However, the advantage of using this low value is to emphasize the non-linear response of the radiative forcing calculation induced by the cloud and aerosol optical thickness variability which is important to determine its sensitivity. The Cloud Optical Depth (COD) is taken from the MODIS cloud product, and the GMAO model was used to determine the vertical profiles of gaseous concentrations and temperatures.

CALIPSO Polarized Observations: Water Cloud Method Principle

Recent developments linked to the CALIPSO mission allowed us to better understand the link between the multiple scattering and the depolarization ratio δ of the laser light in liquid water clouds and its potential applications for space lidar measurements. This link can be expressed by a function f approximately polynomial [7]. In cases where a transparent layer of aerosol lies above a dense liquid water cloud, the layer-integrated attenuated backscatter of the cloud is reduced by a factor that is equal to the two-way transmittance of the upper layer. This two-way transmittance is $T^2 = \exp(-2(\tau_{mL} + \tau_{AL}))$, where τ_{AL} and τ_{mL} are the Aerosol Optical Depth (AOD) and molecular optical depth of the overlying layer, and thus,

$$\tau_{AL} = -\frac{1}{2} \ln(2S_C \gamma_{CL,att} f(\delta)) - \tau_{mL} \quad (3)$$

For water clouds that are measured at 532 nm, the lidar ratio S_C is weakly varying with cloud properties but has a value of around 19 sr [12, 13]. $\gamma_{CL,att}$ is the attenuated backscatter coefficient integrated on the cloud layer [7]. The main source of error in this methodology comes from the lidar calibration error and it can be corrected on area with no aerosols above the cloud. Preliminary comparisons between this method and a different retrieval based on POLDER polarized passive observations [8] show an encouraging level of agreement. Fig. 2 shows the AOD we have used for this study (case of 11 August 2007 around 13TU, in the Gulf of Guinea area). On Fig. 3 we show how we have combined those profiles with the vertical profile of attenuated backscatter coefficient to retrieve the vertical profiles of extinction and give the associated vertical profile of heating rates retrieved by MOMO.

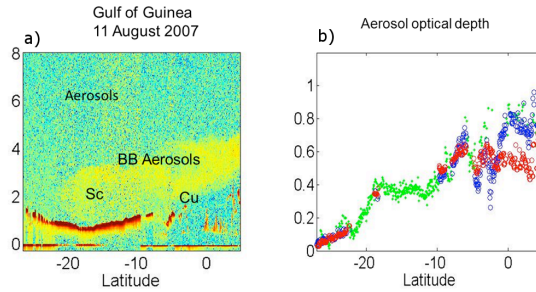


FIGURE 2. a) CALIPSO vertical profile of attenuated backscatter coefficient. b) Red : MODIS, Blue : CALIPSO/CloudSat ocean surface [14, 15], Green : CALIPSO WCM (based on [7]), Polarization based measurements should provide a high accuracy of the retrieval with no assumptions on aerosol microphysical properties (only the signal within the cloud is used). We see a good consistency with MODIS and ocean surface method at cloud boundaries.

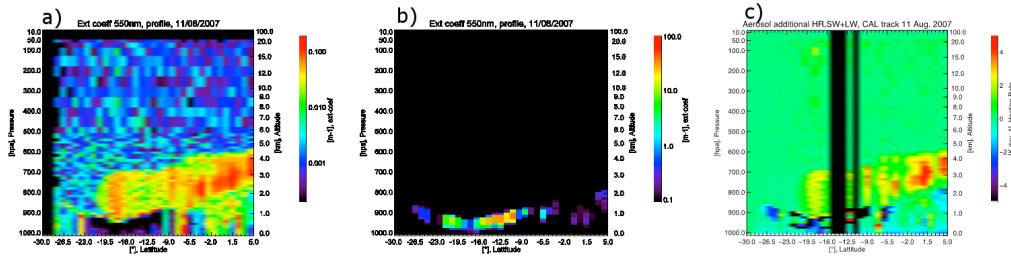


FIGURE 3. a) Vertical profile of aerosol extinction coefficient. b) Vertical profile of cloud extinction coefficient. c) Vertical profile of heating rates associated retrieved by MOMO when those data are used as inputs.

The Imager SEVIRI Onboard Meteosat Second Generation (MSG)

MSG is the new generation of geostationary, meteorological satellites developed by the European Space Agency (ESA) in close co-operation with the European Organisation for the Exploitation of Meteorological Satellites (EUMETSAT). The satellite’s main payload is the optical imaging radiometer so called Spinning Enhanced Visible and Infrared Imager (SEVIRI). Its 12 different spectral channels can provide 20 times more information than previous generation Meteosat satellites, offering new and, in some cases, unique capabilities in cloud imaging and tracking, fog detection, measurement of the earth surface and cloud top temperatures, tracking ozone patterns, as well as many other improved performances. As we can see on Fig. 4, the cloud cover reduces considerably between 7am and 3pm and shows spatial variations. We have chosen to study the effect of cloud variability before to address the effect of advection and sedimentation on the aerosol layer. The reason for this choice is that we expect the cloud cover to vary more quickly at a finer spatial scale and it is the albedo of the cloud below the aerosol layer which determines the sign of the radiative forcing for given aerosol properties. It is important to know the cloud properties at a given time because the forcing does not decrease with the solar flux. The optical thickness of the aerosol layer and its radiative effect are function of the optical path, which increases at low sun elevation. Fig. 5 summarizes a few results that can be drawn from this case study (consistent with the results of [2]).

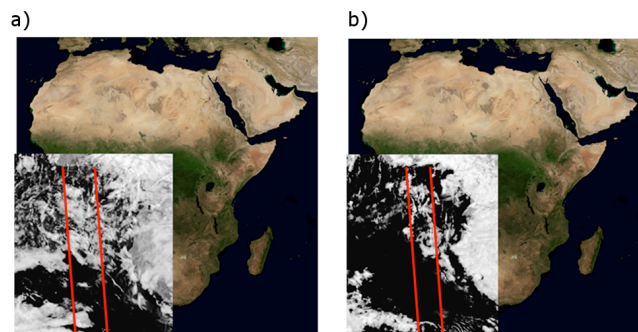


FIGURE 4. SEVIRI reflectances show an important diminution of the cloud cover between a) 7h and b) 15h.

For the same COD and same microphysical properties, higher AOD implies a stronger forcing. For the same AOD and same microphysical properties, COD determines the sign of the forcing and its value. For this case study, a threshold value of 5 in the COD turns the aerosol forcing to positive. In-depth investigations will be required to understand all non-linear processes, the sensitivity to parameters and their variability. A preliminary quantification of cloud coverage variations based on SEVIRI observations shows a +20% evolution during the day. As a first step towards a sensitivity study, we implemented a variation of +30% of the COD to determine the impact on the aerosol forcing and heating rates. It is seen to induce large variations in the forcing as represented in Fig. 5.

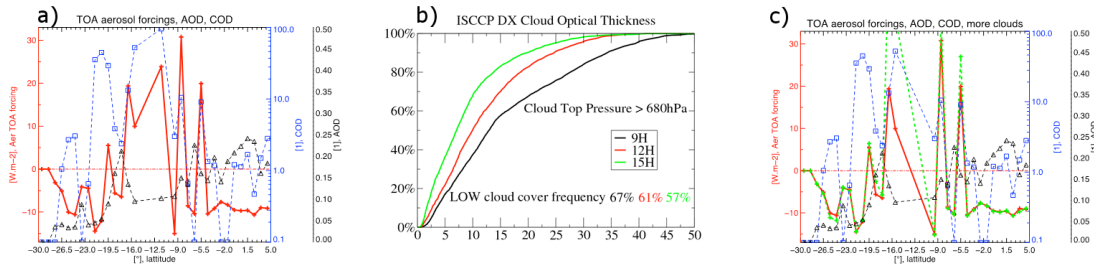


FIGURE 5. a) Top of the Atmosphere (TOA) forcing for the case study represented in Fig. 3. b) Cumulative frequency of cloud optical thickness as retrieved by SEVIRI for this case study at 3 different times, both the probability of cloud cover and cloud optical thickness decreases with time. c) Same as a) with an increase of cloud optical depth by 30% to represent the sensitivity of the radiative forcing to expected cloud optical depth variations.

ACKNOWLEDGMENTS

We gratefully acknowledge the Free University of Berlin, the University Pierre and Marie Curie, SSAI, NASA, CNES, ICARE and its support (CNES, CNRS, the Nord-Pas-De-Calais and the University of Lille) as well as the POLDER, MODIS, CALIPSO, CloudSat, AMSR-E for funding this study and providing data.

REFERENCES

1. J. M. Haywood and K. P. Shine. *Q. J. R. Meteorol. Soc.* **123**, 1907–1930 (1997).
2. J. Haywood and O. Boucher. *Rev. Geophys.* **38**, 4, 513–543 (2000).
3. R. S. Fraser and Y. J. Kaufman, *IEEE Trans. Geosci. Remote Sensing* GE-23, 625 (1985).
4. H. Yu, Y. J. Kaufman, M. Chin, G. Feingold, L. A. Remer, T. L. Anderson, Y. Balkanski, N. Bellouin, O. Boucher, S. Christopher, P. DeCola, R. Kahn, D. Koch, N. Loeb, M. S. Reddy, M. Schulz, T. Takemura and M. Zhou, *Atm. Chem. Phys.* **6**, 613–666 (2006).
5. A. Keil and J. M. Haywood, *J. Geophys. Res.* **108**, D13 (2003).
6. D. Chand, R. Wood, T. L. Anderson, S. K. Satheesh and R. J. Charlson, *Nature Geoscience* **2**, doi:10.1038/NGE0437, 181–184 (2009).
7. Y. Hu, M. Vaughan, Z. Liu, K. Powell and S. Rodier, *IEEE Geosc. Rem. Sens. Lett.* **4**, 523–526 (2007).
8. F. Waquet, J. Riedi, L. C. Labonnote, P. Goloub, B. Cairns, J. L. Deuze and D. Tanre, *J. Atmos. Sci.* **66**, 2468–2480 (2009).
9. F. Fell and J. Fischer, *Rev. Geophys. Space Phys.* **69**, 351–388 (2001).
10. R. Bennartz and J. Fischer, *JQSRT* **66**, 539–553 (2000).
11. M. Hess, P. Koepke and I. Schult, *Bull. Am. Met. Soc.* **79**, 831–844 (1998).
12. R. G. Pinnick, S. G. Jennings, P. Chylek, C. Ham and W. T. Grandy Jr., *J. Geophys. Res.* **88** (C11) 6787–6796 (1983).
13. Y. Hu, M. Vaughan, D. Winker, Z. Liu, V. Noel, L. Bissonnette, G. Roy, M. McGill and C. Trepte, 2006: "A Simple Multiple Scattering-Depolarization Relation And Its Potential Application For Space-based Lidar Calibration", 23rd International Laser Radar Conference (ILRC), Nara, Japan.
14. D. Josset, J. Pelon, A. Protat and C. Flamant, *Geophysical Research Letters* **35**, L10805. doi: 10.1029/2008GL033442 (2008).
15. D. Josset, J. Pelon and Y. Hu, *IEEE Geoscience and Remote Sensing Letters* **7**, 195–199, doi:10.1109/LGRS.2009.2030906 (2010).